



Desynchronization and clustering with pulse stimulations of coupled electrochemical relaxation oscillators

Yumei Zhai^a, István Z. Kiss^{b,*}, Hiroshi Kori^{c,d}, John L. Hudson^a

^a Department of Chemical Engineering, 102 Engineers' Way, University of Virginia, Charlottesville, VA 22904-4741, United States

^b Department of Chemistry, 3501 Laclede Ave., Saint Louis University, St. Louis, MO 63103, United States

^c Division of Advanced Sciences, Ochanomizu Academic Production, Ochanomizu University, Tokyo, Japan

^d PRESTO, Japan Science and Technology Agency, Kawaguchi, Japan

ARTICLE INFO

Article history:

Available online 12 June 2009

Keywords:

Desynchronization
Pulse
Phase model
Electrochemical oscillation

ABSTRACT

Effects of pulse stimulations on the dynamics of relaxation oscillator populations were experimentally studied in a globally coupled electrochemical system. Similar to smooth oscillations, weakly and moderately relaxational oscillations possess a vulnerable phase, ϕ_S ; pulses applied at ϕ_S resulted in desynchronization followed by a return to the synchronized state. In contrast to smooth oscillators, weakly and moderately relaxational oscillators exhibited transient and itinerant cluster dynamics, respectively. With strongly relaxational oscillators the pulse applied at a vulnerable phase effected transitions to other cluster configurations without effective desynchronization. Repeated pulse administration resulted in a cluster state that is stable against the perturbation; the cluster configuration is specific to the pulse administered at the vulnerable phase. The pulse-induced transient clusters are interpreted with a phase model that includes first and second harmonics in the interaction function and exhibits saddle type cluster states with strongly stable intra-cluster and weakly unstable inter-cluster modes.

© 2009 Elsevier B.V. All rights reserved.

1. Introduction

Synchronized populations of oscillators abound in a variety of fields including physics [1], chemistry [2], biology [3–5], neuroscience [6], and medicine [7]. The collective behavior of entrained oscillators can be affected and controlled not only by mutual coupling among the individual elements [2] but also by external stimuli such as feedback [8,9] and pulse stimulations [7].

Theoretical and experimental studies on the effects of pulse stimulations in relaxation oscillator populations have relevance to the behavior of biological rhythms: pacemaker cells often exhibit relaxation oscillations [3]. Stable clustering behavior is possible in systems of coupled phase oscillators [10–13] and chemical [14–16] and electrochemical experiments [17–19] as well. The effects of pulse stimulations of uniformly synchronized relaxation oscillator populations could reveal transient cluster dynamics that are difficult to predict from stable behavior.

Pulse stimulations including single pulse [7], double pulse [20], and bipolar double pulse [21] methods, have been proposed for desynchronization in studies of coupled phase oscillators because

of their possible application in medical treatment of some diseases associated with pathological synchronization of neurons. Depending on the phase, a pulse may either advance or delay the oscillation. Hence, desynchronization can be achieved with a single pulse stimulation of the right intensity and duration by hitting the synchronized system in a vulnerable phase in such a way that approximately half of the elements are delayed, whereas the elements in the other half are advanced. The approximate position of the vulnerable phase is expected to occur at a phase where the phase response function has large positive slope; however, the exact position depends on the coupling strength (level of synchrony) and on the nature of oscillators and their heterogeneities [3,7].

The effect of pulse stimulation on desynchronization of a population of smooth oscillators has been previously investigated experimentally [22]. With a laboratory electrochemical reaction system that exhibits transient dynamics, heterogeneities, and inherent noise, we have shown that stimulation with a short, single pulse applied at a vulnerable phase can effectively desynchronize a cluster of smooth oscillators [22]. In addition, we showed in the experiments that the double pulse method, that can be applied at any phase, can be improved either by adding an extra weak pulse between the original two pulses or by adding noise to the first pulse.

In this paper, we apply pulse stimulations in ordered populations of relaxation electrochemical oscillators to investigate the

* Corresponding author. Tel.: +1 314 977 2139; fax: +1 314 977 2521.

E-mail addresses: izkiss@slu.edu (I.Z. Kiss), hudson@virginia.edu (J.L. Hudson).

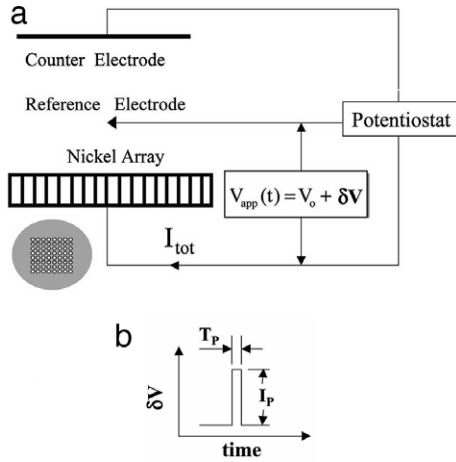


Fig. 1. (a) Schematic of apparatus with pulse stimulations (δV). (b) A single pulse signal with pulse duration T_p and intensity I_p .

differences of desynchronization properties of smooth and relaxation oscillators. The effects of pulse stimulations on the collective oscillations (or the degree of synchronization) and clustering are experimentally investigated for weakly, moderately, and strongly relaxational oscillators. The observed transient clusters are qualitatively interpreted with a globally coupled phase model that contains first and second harmonics in the interaction function.

2. Experimental

The experiments were carried out with an array of electrodes as shown in Fig. 1a.

A standard electrochemical cell consisting of a nickel working electrode array (64 1-mm diameter electrodes with an 8×8 configuration), Hg/Hg₂SO₄/cc.K₂SO₄ reference electrode, and a platinum mesh counter electrode was used. Experiments were carried out in 3 mol/L sulfuric acid solution at a temperature of 11 °C. The working electrodes are embedded in epoxy, and reaction takes place only at the ends. A constant potential (V_0 vs. the reference electrode) is applied to all electrodes through a potentiostat. The pulse perturbation signal (δV) is superimposed on V_0 via the potentiostat. Real-time Labview was used to visualize and save the individual current data on a computer as well as to generate pulses (Fig. 1b) to be applied by the potentiostat. The sampling rate was 200 Hz. Since the currents of all the individual electrodes are measured, the rate of reaction as a function of position and time is obtained.

The electrodes were connected to the potentiostat through 64 uniform individual resistors connected to each of the electrode (R_{ind}) and one collective resistor (R_{coll}) (not shown in the figure). The collective resistor couples the electrodes globally [17,23]. We employed a method of altering the strength of global coupling while holding other parameters constant [23], in which the total external resistance ($R_{tot} = R_{coll} + R_{ind}/N = 10.2 \Omega$) was held constant while the fraction dedicated to individual currents, as opposed to the total current, was varied. A global coupling parameter, defined as $\varepsilon = R_{coll}/R_{tot}$, takes on values from zero to one for the zero to strongest added global coupling case.

The current of a single electrode becomes oscillatory at about $V_0 \cong 1.05$ V where a Hopf bifurcation takes place [17]. The oscillations cease at $V_0 \cong 1.30$ V with a saddle-loop bifurcation, below which there is a region of relaxation oscillations where the angular velocity varies with time [17,18]. A representative time series of the relaxation oscillations is shown in Fig. 2; a slowing down at the minimum values of the current can be seen. The Hilbert transform, $h[I(t) - \langle I \rangle]$, where $I(t)$ is the current and $\langle I \rangle$

is its temporal mean, is used to construct the phase space and to obtain the phase of an individual oscillator [24,25]. The limit cycle in the 2D phase space ($h[I(t) - \langle I \rangle]$ vs. $[I(t) - \langle I \rangle]$) for the relaxation oscillator is presented in Fig. 2b. The phase at time t is obtained as the angle ϕ in Fig. 2b. $\phi = 0$ corresponds to the maximum current in a cycle. The phase as a function of time is shown in Fig. 2c. Without added global coupling, the points on a snapshot in the 2D phase space for the 64 oscillators are well distributed on the limit cycle (Fig. 2d); this indicates a lack of synchrony. The frequency distribution of the uncoupled relaxation oscillators is nearly unimodal and relatively flat; the standard deviation of the frequencies is about 10% of the 0.4 Hz mean frequency [26]. An order parameter similar to the Kuramoto order [26] defined as

$$r = \frac{|\sum_j P_j(t)|}{\sum_j |P_j(t)|} \quad (1)$$

is used to characterize the degree of synchronization, where $P_j(t)$ is the vector of the element j in Fig. 2d.

A (nearly) phase synchronized state was obtained at the beginning of the experiments by increasing the global coupling strength in the population [26,25,27].

We use the average distance clustering algorithm of Matlab to construct hierarchical cluster trees from experimental data. The dynamics are reconstructed for each element using time delay coordinates (delay time: 0.2 s, embedding dimension: 3). At selected M times (here $M = \lceil 200 \times T_0 \rceil$, where T_0 is the period of the mean current in seconds) the three state space coordinates of each element are recorded. The j th observation of the k th element is $\mathbf{x}_{j,k}$, where $\mathbf{x}_{j,k}$ is a 3D vector, $j = 1 \dots M$, $k = 1 \dots 64$. The distances ($\delta_{k,l}$) among the observation vectors ($\mathbf{X}_k = \{\mathbf{x}_{1,k}, \mathbf{x}_{2,k}, \dots, \mathbf{x}_{M,k}\}$) of each pair of elements in the $M \times 3$ -dimensional space are determined ($\delta_{k,l} = |\mathbf{X}_k - \mathbf{X}_l|$) and a cluster tree is constructed using an average distance algorithm. Element k is classified to belong to cluster of set of elements with precision E if $|\mathbf{X}_k - \bar{\mathbf{X}}| < E$, where $\bar{\mathbf{X}}$ is the mean value of observation vectors of the cluster. The number of points at a given clustering distance (E) shows the number of clusters to within that precision. The plots consist of many inverted U-shaped lines connecting the different clusters in a hierarchical tree such as that shown in Fig. 3d.

3. Results

3.1. Desynchronization and transient clustering of weakly relaxational oscillators

At $V_0 = 1.215$ V, the oscillation of the individual current is weakly relaxational as the applied potential is still far away from the saddle-loop bifurcation point ($V_0 \cong 1.30$ V). With an added global coupling of $\varepsilon = 0.2$, a highly synchronized state with a mean order of $\langle r \rangle = 0.99$ was obtained for the relaxational oscillator population. The period of the collective signal, the mean current, was about $T_0 = 2.14$ s.

Similar to the pulse stimulations on populations of smooth electrochemical oscillators [22], we found there exists a vulnerable phase of the collective oscillator such that the collective oscillations can be effectively suppressed through desynchronization if the pulse is administered at this specific time. The vulnerable phase was $\phi_S = \phi'/(2\pi) = 0.35$ for synchronized smooth oscillators with a pulse of $\{I_p, T_p\} = \{-0.6$ V, 0.1 s} [22], where ϕ' is the phase where the stimulation was applied in radians. For the synchronized weakly relaxational oscillators, the vulnerable phase was shifted to $\phi_S = 0.99$. When the pulse is administered at other phases, as in the case of smooth populations, either slightly enhanced synchronization (with higher order) or no significant changes of the

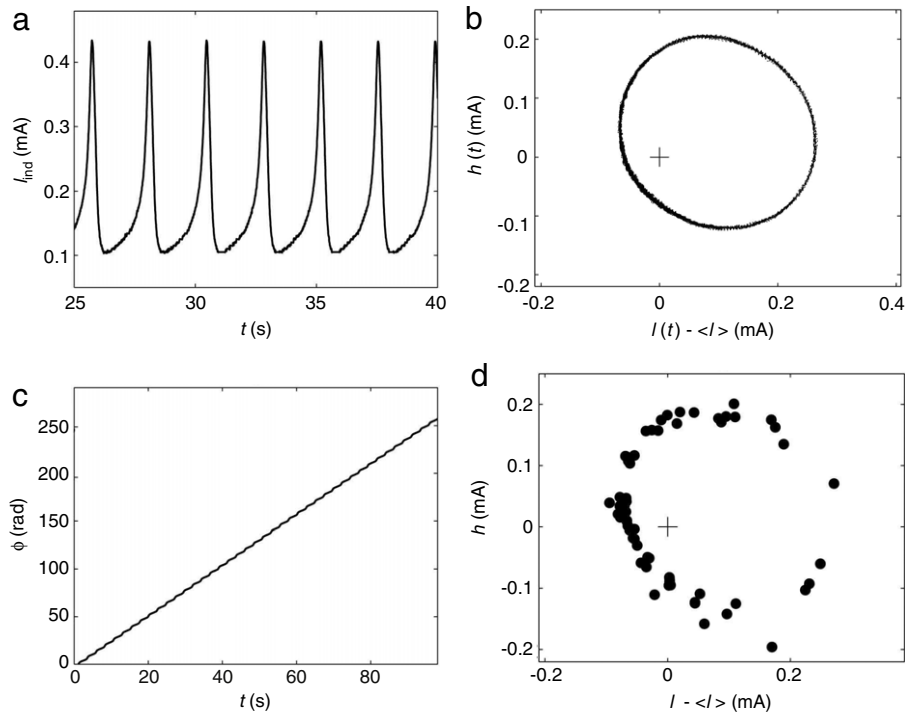


Fig. 2. Dynamics of uncoupled 64 relaxation electrochemical oscillators. (a) Time series of a single electrode current. (b) Phase portrait of a single oscillator with Hilbert transform. (c) Phase of a single oscillator vs. time. (d) Snapshot of the 64 oscillators in the phase space. $V_0 = 1.215$ V. The symbol ‘+’ denotes the origin (center of rotation).

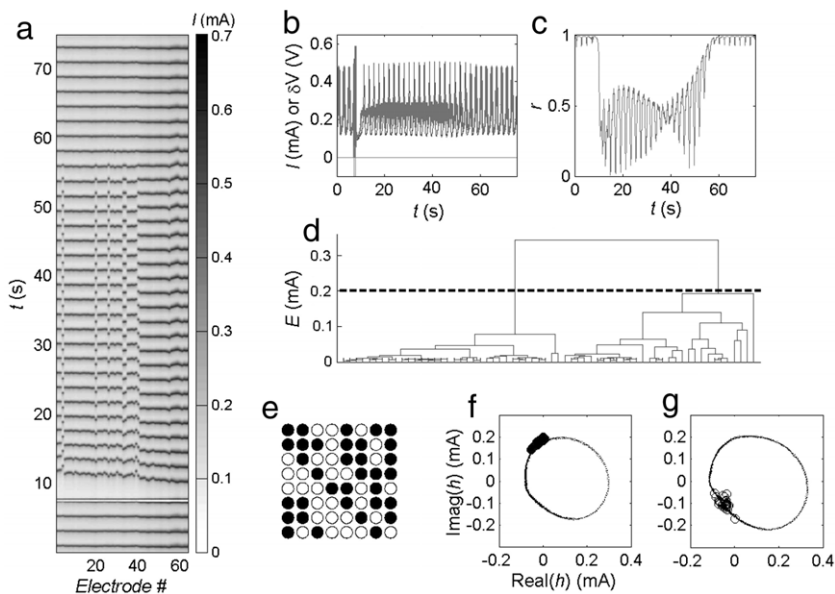


Fig. 3. Suppression of synchrony of a highly synchronized population of weakly relaxational oscillators with pulse stimulation. $V_0 = 1.215$ V, $\varepsilon = 0.2$, $T_0 = 2.14$ s. The pulse ($\{I_p, T_p\} = \{-0.6$ V, 0.35 s}) was applied around $t = 7.5$ s when $\phi_s = 0.99$, before which the mean order $r_0 = 0.99$. (a) Grayscale plot of individual currents. (The elements are ordered by their intrinsic frequencies from low to high.) (b) Time series of mean current (bold line), individual current (thin line) and stimulation signal. (c) Time series of order. (d) Hierarchical cluster tree obtained with time series data from $t = 40$ s to $40 + T_0$ s. (e) Cluster configuration on the array at $t = 40$ s. (f, g) Snapshots of phase points of the two clusters in the 2D phase space. Circles: phase points at $t = 40$ s. Dots: trajectory of one typical individual element.

collective behavior is observed. The suppression of the synchrony by a pulse of $\{I_p, T_p\} = \{-0.6$ V, 0.35 s} applied at $\phi_s = 0.99$ is presented in Fig. 3.

The grayscale plot of all the individual currents (Fig. 3a) shows that the uniform dynamics of the system were destroyed when the pulse was administered at about $t = 7.5$ s; all the elements remained oscillatory but their phases were no longer locked for about 23 cycles (50 s) after the pulse. With a closer look at the grayscale plot of the currents we can see that the pulse induced transient clusters in the system. The time series of the currents in

Fig. 3b shows that after the pulse stimulation, the amplitudes of the mean signal (bold line) was significantly decreased while those of the individual currents maintained their original large values (thin line). The instantaneous order was reduced to nearly half of that before the pulse stimulation with a mean value about 0.5 as the result of the pulse stimulation (Fig. 3c). Because the clusters were unstable, the resulted desynchronization was transient as well. Resynchronization gradually developed as the clustering disappeared for $t > 50$ s. The hierarchical cluster tree in Fig. 3d shows that with a precision of $E = 0.2$ mA the system can be

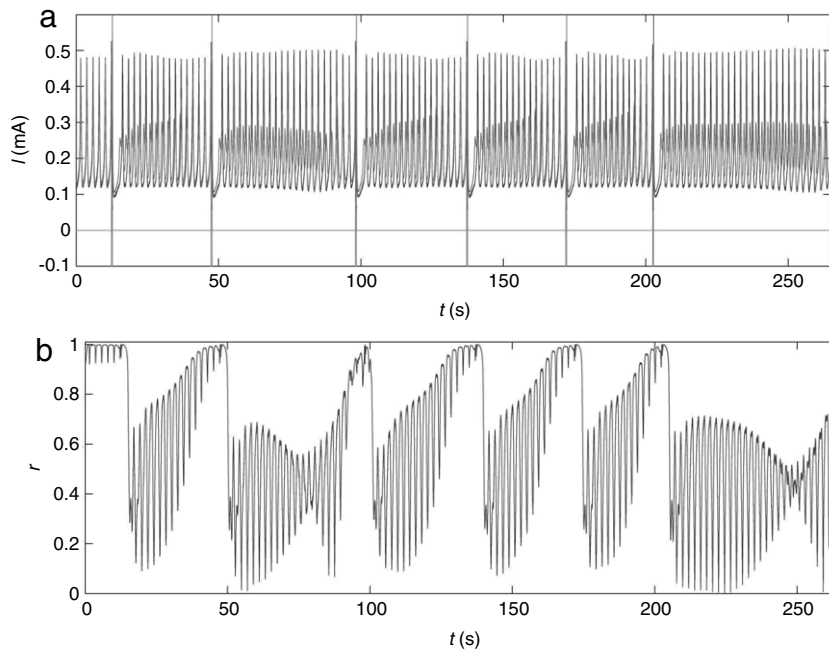


Fig. 4. Repeated single pulse stimulation in a synchronized population of weakly relaxational oscillators. The experimental conditions were the same as in Fig. 3. The pulse $\{I_p, T_p\} = \{-0.6 \text{ V}, 0.3 \text{ s}\}$ was applied at $\phi_s = 0.99$ once the mean current reached an threshold value $A_T = 0.45 \text{ mA}$. The stimulation started at $t_s = 10 \text{ s}$. The mean orders before and after t_s were $r_0 = 0.99$ and $r_1 = 0.62$, respectively. The average frequency of the pulse administration $f_s \approx 4.0/100$ cycles. (a) Time series of mean current (bold line), individual current (thin line) and stimulation signal. (b) Time series of order.

considered to contain two clusters during the desynchronization. The cluster configuration (Fig. 3e) was quite balanced (34, 30), where black circles stand for the cluster of 34 elements and the hollow circles for the other cluster. The snapshot of the phase points of the elements in each cluster is presented along with a typical trajectory in Fig. 3f and g, respectively. There was a small difference in the amplitudes of the oscillations that belonged to different clusters; the oscillations in the slightly larger cluster had smaller amplitudes.

As described above, for weakly relaxational oscillators, the cluster state induced by a pulse at the vulnerable phase is unstable and after some time merging of the clusters will occur. Repeated application of the single pulse thus is required to maintain the low-order state. Fig. 4 shows the results of demand-controlled repeated single pulse experiments in the weakly relaxational population. Before the stimulation the mean order was $r_0 = 0.99$ and during the control the mean order was decreased to 0.62. There was variability in the series of desynchronization steps. This is likely due to the sensitive dependence of the narrow vulnerable phase range on instantaneous order and on minor variations of the system conditions [22]. The average frequency of the pulse administration $f_s \approx 4.0/100$ cycles. It is expected that with a lower initial order and an optimized threshold for the pulse triggering a lower order can be obtained with repeated single pulse stimulations.

3.2. Itinerant clusters of moderately relaxational oscillators

When the applied potential is set at $V_0 = 1.265 \text{ V}$, the individual oscillations are more relaxational because the system is closer to the saddle-loop bifurcation point. We refer to the oscillator obtained at this potential as ‘moderately’ relaxational [18]. With an added coupling of $\varepsilon = 0.6$, the population was fairly synchronized with a mean order of $r_0 = 0.90$ and the period of the mean current was $T_0 = 2.62 \text{ s}$.

In Fig. 5, we show that after a single pulse of $\{I_p, T_p\} = \{-1 \text{ V}, 1 \text{ s}\}$ itinerant clusters formed; the transient dynamics are

characterized by alternating formation and destruction of various cluster states. The vulnerable phase was $\phi_s = 0.51$. In the grayscale plot of individual currents (Fig. 5a) the clustering state can be recognized before $t = 110 \text{ s}$, after which it was eventually replaced with a one-cluster state similar to that before the pulse stimulation. A temporary return to a higher-order state occurred at around $t = 50 \text{ s}$. The time series of the mean current (Fig. 5b) and the order (Fig. 5c) further reflect the existence of the itinerant clusters. One larger mean oscillation was seen at $t = 50 \text{ s}$ when the cluster state gave way to a synchronized state for a short time (Fig. 5b). The order switched between a state of a low mean value with large variations and another state of a high mean value with smaller variations before $t = 110 \text{ s}$, after which it permanently stayed in the latter state (Fig. 5c). The clustering analysis (Fig. 5d–e) shows that the itinerant clusters obtained after the pulse stimulation was highly unbalanced two-cluster with the configuration of (51, 12) (with one element ‘off’). Again, the elements in the larger cluster oscillated with smaller amplitudes (Fig. 5f) while those in the smaller cluster oscillated with larger amplitudes (Fig. 5g). Compared with the transient clustering state obtained with pulse stimulations in weakly relaxational oscillators (Fig. 3f and g), the difference in the trajectories of typical oscillators in each of the two clusters were more evident in this highly unbalanced state.

3.3. Transitions among clusters with strongly relaxational oscillators

We then increased the applied potential to $V_0 = 1.285 \text{ V}$, which is close to the saddle-loop bifurcation point of $V_0 = 1.300 \text{ V}$. The individual oscillation obtained at this potential is ‘strongly’ relaxational and the one-cluster state is not stable [18]. However, at $\varepsilon = 0.6$ a three-cluster state with large order parameter $\langle r \rangle = 0.92$ was attained. Pulse stimulation of this cluster state at a specific phase of $\phi_s = 0.51$ leads to other cluster states rather than effective desynchronization. Unlike in the experiments on a weakly or moderately relaxational population, the new cluster states are stable once they are induced by pulse stimulations.

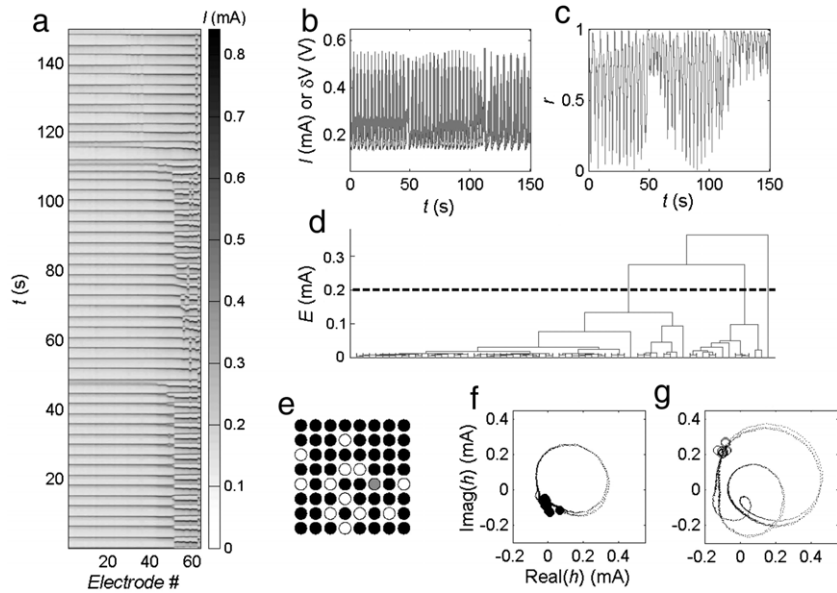


Fig. 5. Itinerant clusters formed after a single pulse stimulation in an ordered population of moderately relaxational electrochemical oscillators. $V_0 = 1.265$ V, $\varepsilon = 0.6$, $T_0 = 2.62$ s. The pulse of $\{I_p, T_p\} = \{-1$ V, 1 s $\}$ was applied at $\phi_S = 0.51$. Before the pulse stimulation $r_0 = 0.90$. (a) Grayscale plot of individual currents. (b) Time series of mean current (bold line) and individual current (thin line). (c) Time series of order. (d) Hierarchical cluster tree obtained with time series data from $t = 20$ s to $20 + T_0$ s. (e) Cluster configuration on the array at $t = 20$ s. (f, g) Snapshot of phase points in the 2D phase space at $t = 20$ s.

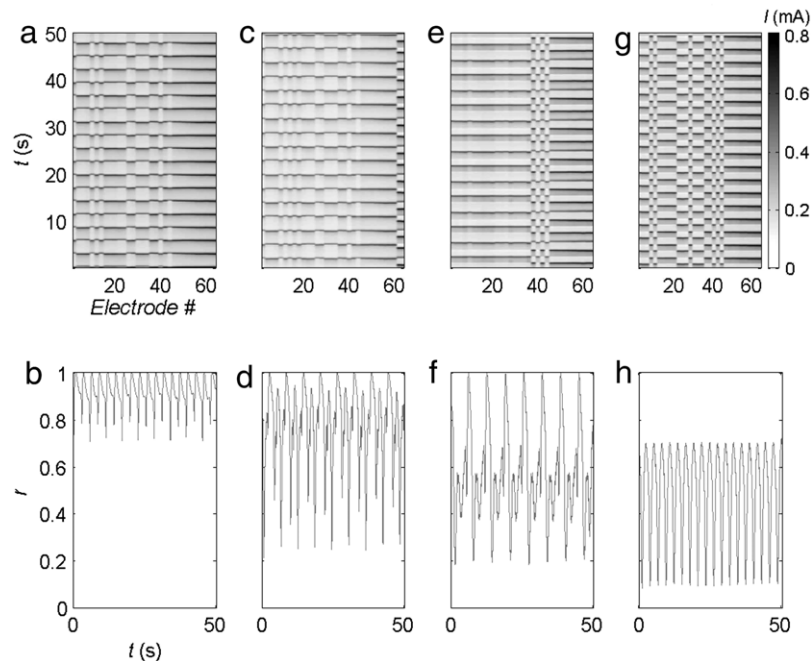


Fig. 6. Pulse stimulations in an ordered population of strongly relaxational electrochemical oscillators. $V_0 = 1.285$ V, $\varepsilon = 0.6$, $T_0 = 2.87$ s. The pulse was applied at $\phi_S = 0.51$. Top row: Grayscale plots of individual currents. Bottom row: Time series of order. (a)–(b) Stable clusters before pulse stimulations (State I). The mean order $\langle r \rangle = 0.92$. (c)–(d) New stable cluster induced with a single weak pulse stimulation (State II). $\{I_p, T_p\} = \{-0.6$ V, 0.25 s $\}$. $\langle r \rangle = 0.78$. (e)–(f) Stable two-cluster state (State III) obtained after the second or more administration of the weak pulse. $\langle r \rangle = 0.57$. (g)–(h) Another stable two-cluster state (State IV) obtained with a single pulse stimulation of $\{I_p, T_p\} = \{-1$ V, 0.5 s $\}$ from a state similar to State I. $\langle r \rangle = 0.49$.

The top row of Fig. 6 shows the grayscale plots of individual currents of an ordered strongly relaxational population before and after pulse stimulations; corresponding cluster analyses and 2D state space embeddings are shown in Fig. 7. A three-cluster state (State I) was attained before pulse stimulations (Fig. 6a). The elements with lower intrinsic frequencies formed two anti-phase period-2 clusters while those whose oscillations were more regular formed a third cluster at the higher intrinsic frequency region. After a weak pulse of $\{I_p, T_p\} = \{-0.6$ V, 0.25 s $\}$ applied at $\phi_S = 0.51$, a small, new period-2 cluster (with 4 elements)

appeared at the high intrinsic frequency side while most remaining elements were kept in their respective clusters (Fig. 6c, State II). The experimental system was perturbed again with the same weak pulse at $\phi_S = 0.51$. After the 2nd perturbation the new cluster at the high intrinsic frequency side expanded its size and other elements of the lower intrinsic frequencies formed a single cluster that is anti-phase with the other (State III, Fig. 6e). Note that the local dynamics in this two-cluster state are different than those in State I, before the pulse stimulation. The system remained in

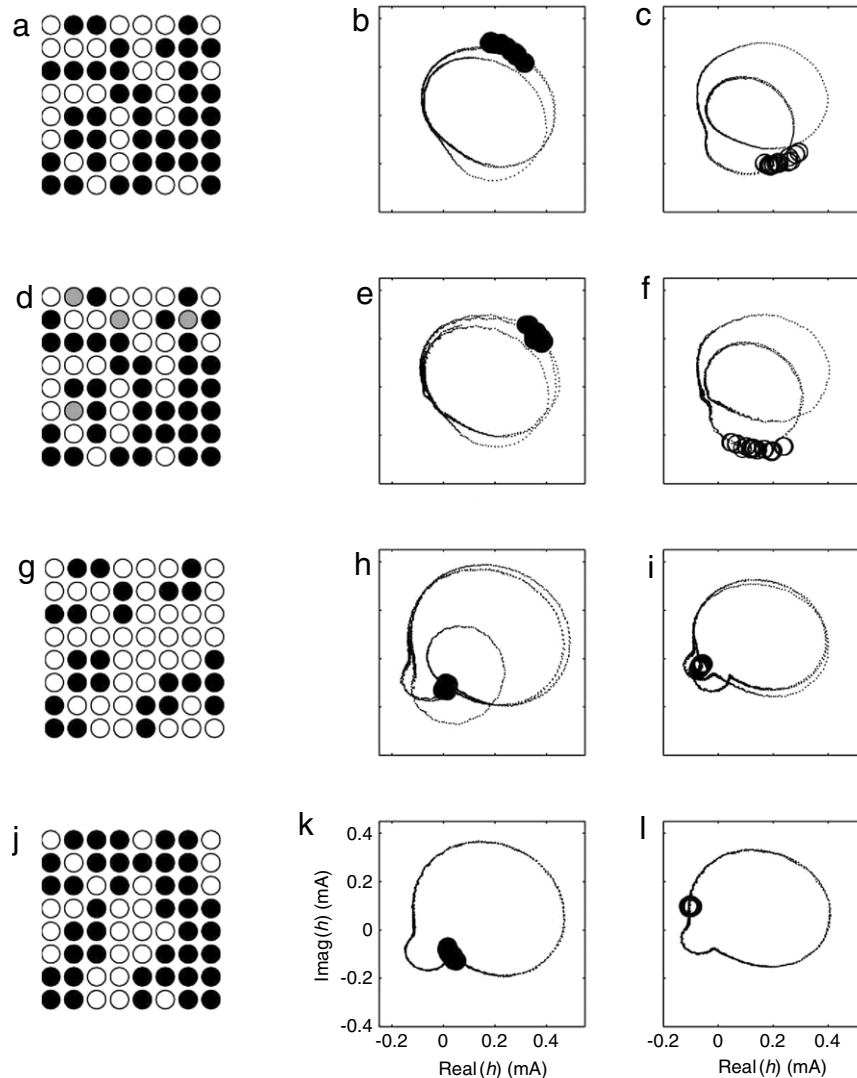


Fig. 7. Cluster analysis of data in Fig. 6. Left column: Cluster configurations on the array. Middle column: Snapshots of phase points (circles) of elements that are filled in black in the configuration plot and a typical trajectory in this cluster. Dots: Trajectory of a typical oscillator in the respective cluster. Right column: Snapshots of phase points of the elements that are hollow in the configuration plot and a typical trajectory in this cluster. (a)–(c) State I, before pulse stimulation. The mean order (r) = 0.92. (With a precision of $E = 0.18$ mA applied here only two of the three clusters shown in Fig. 6a can be resolved; with lower error we do obtain three clusters.) (d)–(f) State II, after a single weak pulse stimulation. $\{I_p, T_p\} = \{-0.6$ V, 0.25 s). (r) = 0.78. (g)–(i) State III, after the second administration of the weak pulse. (r) = 0.57. (j)–(l) State IV, after a single pulse stimulation of $\{I_p, T_p\} = \{-1$ V, 0.5 s) from a state similar to State I. (r) = 0.49.

State III after subsequent administrations of the weak pulse at $\phi_s = 0.51$.

The shown new clustering states (State II and III) were neither observed ‘naturally’ with the change of global coupling nor with perturbations through opening the circuit. Instead, they could be induced by pulse stimulations applied at a specific time (the vulnerable phase $\phi_s = 0.51$). When the pulse was applied at another time, the system returned to a state similar to State I.

A stable final state that is specific to a pulse administered at the vulnerable phase can be attained. For example, another anti-phase two-cluster state was observed with a stronger pulse of $\{I_p, T_p\} = \{-1$ V, 0.5 s), as shown in Fig. 6g. Similar to those in State III obtained with a weak pulse, all the individual oscillations became period-2 after the strong pulse stimulation. Again, if the pulse is applied at a non-vulnerable phase, the system will resume a state similar to State I.

The collective behavior of the system is greatly affected by pulse stimulations. The bottom row of Fig. 6 shows the time series of a collective signal of the system, the order. Before any pulse

stimulations or if the pulse was applied at non-vulnerable phases, the order had a high mean value (0.92) with relatively small-amplitude period-2 oscillations (Fig. 6b). A lower mean order of 0.78 was obtained in State II, when only a few elements were in the new cluster state induced by a single perturbation with the weak pulse of $\{I_p, T_p\} = \{-0.6$ V, 0.25 s) (Fig. 6d). The order started to exhibit large variations of period-3 because of the appearance of a new, small cluster. At the final clustering state induced with the weak pulse, the order was even lower (0.57) with large period-3 oscillations (Fig. 6f). After a single stronger pulse stimulation with $\{I_p, T_p\} = \{-1$ V, 0.5 s), the order exhibited regular periodic oscillations with a mean of 0.49 (Fig. 6h).

3.4. Interpretation of transient clustering with phase models

A characteristic feature of the experimental results is the appearance of transient cluster dynamics during the resynchronization process; we observed a transient two-cluster state with

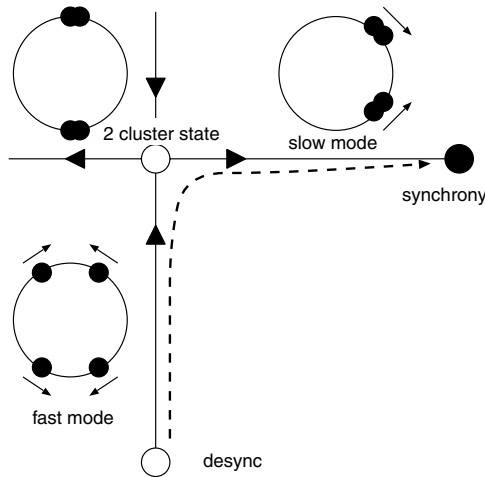


Fig. 8. Phase space structure for a model exhibiting transient clusters.

weakly relaxational oscillators. To interpret the qualitative features of the transient cluster dynamics, we develop a phase model with which transient clusters observed with weakly relaxational oscillators can be described.

A phase model description has been successfully applied to describe (stationary) cluster formation in the electrochemical system due to coupling in previous studies [18,28]. The experiment-based phase models confirmed that the smooth oscillators have predominantly first harmonic ($\sin(\Delta\phi)$) odd components in the interaction function; for relaxational oscillators second harmonics appear. Therefore, to simulate the experimentally observed transient behavior induced by pulses, we investigate the transients to the one-cluster state for a phase model with strong $\sin(\Delta\phi)$ and relatively weak $\sin(2\Delta\phi)$ components.

When the system is in the globally stable one-cluster state, by giving a carefully tuned pulsing to all the oscillators, an almost desynchronized state is obtained in which the phases are nearly homogeneously distributed. From almost desynchronized states the system typically approaches two-cluster states (where one can observe well-defined two clusters for a long time) before the one-cluster attractor is reached. Such a scenario can be interpreted by assuming that the two-cluster state is a saddle solution with strongly stable intra-cluster modes and weakly unstable inter-cluster modes (See Fig. 8). The two-cluster states thus form from an almost desynchronized state by moving along the (fast) stable intra-cluster modes; the two-cluster state is destroyed by moving along the slow inter-cluster mode by decreasing the phase difference among the groups and finally reaching the one-cluster state.

Because previous studies dealing with the realization of desynchronous states by pulsing have already clarified its mechanism [29,7], we focus on validating our assumptions about transient clustering. We thus take an almost desynchronized state as an initial condition and observe its trajectory. A small system size ($N = 4$) is first considered, where the dynamical behavior is better understood. We then investigate the system with a large population to check whether the same scenario holds for a large system.

We introduce a mathematical model with the form:

$$\dot{\phi}_i = \omega + \frac{K}{N} \sum_{j=1}^N H(\phi_j - \phi_i), \quad (2)$$

where ϕ_i is the phase of oscillator i ($i = 1, 2, \dots, N$), ω natural frequency (identical for all the oscillators), K coupling strength, and $H(\Delta\phi)$ the phase interaction function given by

$$H(\Delta\phi) = a \sin(\Delta\phi) + b \sin(2\Delta\phi). \quad (3)$$

By applying a rotating frame and rescaling time scale, we put $\omega = 0$, $K = 1$, and $|a| = 1$ without loss of generality. (For Eq. (2) with general $H(\Delta\phi)$ the existence and stability condition of various cluster states has been studied by Okuda [10].)

We first consider $N = 4$. There are four types of phase locking (i.e., steady) states for this case, namely, (i) one-cluster state: $\phi_1 = \phi_2 = \phi_3 = \phi_4$, (ii) desynchrony: $\phi_1 = \phi_2 + \pi/2 = \phi_3 + \pi = \phi_4 + 3\pi/2$, (iii) two-cluster state (2, 2): $\phi_1 = \phi_2 = \phi_3 + \pi = \phi_4 + \pi$, (iv) two-cluster state (3, 1): $\phi_1 = \phi_2 = \phi_3 = \phi_4 + \pi$. Here we have represented only one configuration for each of the states (ii)–(iv) for simplicity. The stabilities of these states are found as follows. We introduce small deviations $\delta\vec{\phi} = (\delta\phi_1, \delta\phi_2, \delta\phi_3, \delta\phi_4)$ given by $\delta\phi_i = \phi_i - \phi_i^0$ where ϕ_i^0 is a phase locking solution. By linearizing Eq. (2) and solving the eigenvalue problem for the stability matrix, we obtain the following properties:

- (i) one-cluster state: $\lambda^{(i)} = -a - 2b$ (multiplicity 3) with a corresponding eigenvector, e.g., $\delta\vec{\phi} = (1, -1, 0, 0)$
- (ii) desynchronized state: $\lambda_1^{(ii)} = a/2$ (multiplicity 2) with the corresponding eigenvectors $(1, 0, -1, 0)$ and $(0, 1, 0, -1)$; $\lambda_2^{(ii)} = 2b$ (multiplicity 1) with the corresponding eigenvector $(1, -1, 1, -1)$
- (iii) two-cluster state (2, 2): $\lambda_1^{(iii)} = a - 2b$ (multiplicity 1) with the eigenvector $(1, 1, -1, -1)$, namely, the inter-cluster mode; $\lambda_2^{(iii)} = -2b$ (multiplicity 1) with the eigenvector $(1, -1, 0, 0)$ and $\lambda_3^{(iii)} = -2b$ (multiplicity 1) with the eigenvector $(0, 0, 1, -1)$, which are the intra-cluster modes
- (iv) two-cluster state (3, 1): $\lambda_1^{(iv)} = a - 2b$ (multiplicity 1) with the eigenvector $(1, 1, 1, -3)$, namely, the inter-cluster mode; $\lambda_2^{(iv)} = -2b - a/2$ (multiplicity 2) with the eigenvector, e.g., $(1, -1, 0, 0)$, namely, one of the intra-cluster modes.

Note that every state has an additional zero eigenvalue with $\delta\vec{\phi} = (1, 1, 1, 1)$, which is irrelevant to our argument.

Next, we numerically investigate Eq. (2). The parameter values are chosen according to our assumptions: $\lambda^{(i)} = -a - 2b$ is negative; $\lambda_1^{(iii)} = a - 2b$ is small positive; $\lambda_2^{(iii)} = -2b$ is negative. We thus set $a = 1$ and $b = 0.49$. This particular choice makes the desynchronized state unstable, which is also a required property. To visualize trajectories, we introduce two order parameters: $R_1 = |1/N \sum_j \exp(i\phi_j)|$ and $R_2 = |1/N \sum_j \exp(2i\phi_j)|$. In (R_1, R_2) space, each state assumes the following value: (i) (1, 1), (ii) (0, 0), (iii) (0, 1), and (iv) (0.5, 1). We assume almost desynchronized states as initial conditions, given by $\phi_i = 2i\pi/N + \epsilon\xi_i$ where ξ_i is a random number independently taken from the uniform distribution (0, 1) and $\epsilon = 0.01$. Fig. 9a and b display two particular trajectories. In Fig. 9a, the system evolves quickly along the intra-cluster modes of the state (iii), and thus, well defined two clusters are formed. Then, along the inter-cluster mode (the manifold of which is shown by dotted line), two clusters slowly get closer to approach the state (i). Note that the trajectory seems to approach the point $(1/\sqrt{2}, 0)$. This corresponds to the state where two clusters are separated by $\pi/2$, which is not a fixed point and the system smoothly passes it. In Fig. 9b, the system evolves along the intra-cluster modes of state (iv), which is followed by the formation of the unbalanced two clusters. Eventually the system converges to state (i). Fig. 9c displays trajectories starting from 50 different initial conditions. As seen, most trajectories approaches the state (iii). Thus, typically, the balanced two clusters are formed.

We then consider $N = 64$ with the same interaction function, i.e., Eq. (3). The existence and stability conditions for the one-cluster [state(i)] and desynchronized [state(ii)] states are the same as for $N = 4$. There are many two-cluster states for $N = 64$ with various population ratios; we denote the two-cluster state in which one of the clusters is composed of N_1 oscillators by $(N_1, N -$

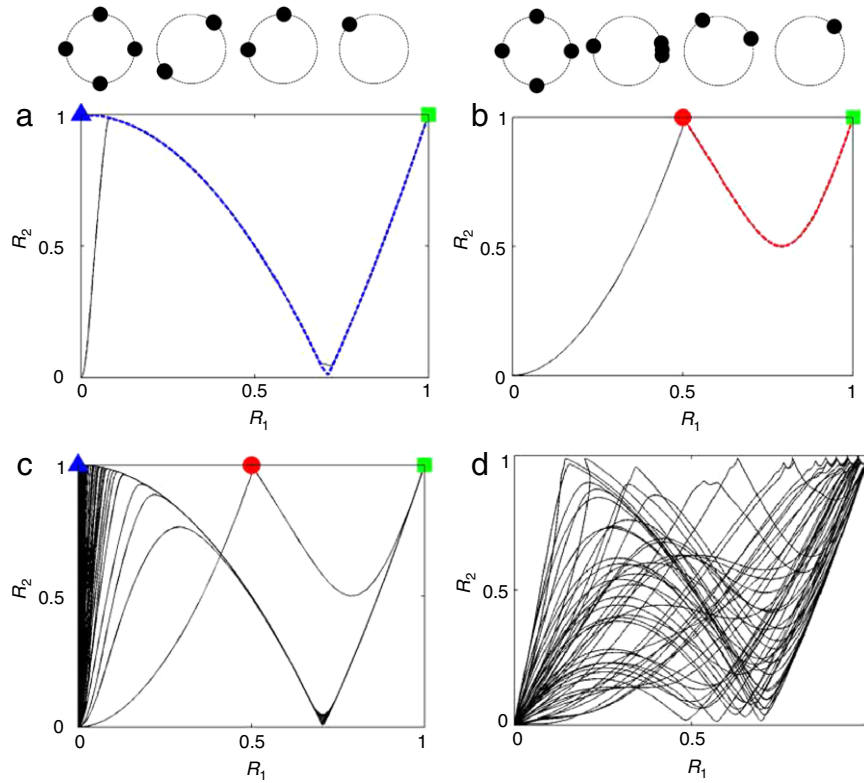


Fig. 9. Numerically obtained trajectories of the phase model in (R_1, R_2) space. Initial conditions are set to almost desynchronized states. The system size is $N = 4$ except for (d) where $N = 64$. (a) A particular trajectory approaching state (i) through the neighborhood of state (iii). Square: state (i), triangle: state (iii). The dotted line shows the inter-cluster manifold of the state (iii). (b) A particular trajectory approaching state (i) through state (iv) denoted by a circle. The dotted line shows the inter-cluster manifold of the state (iv). (c) Trajectories starting from 50 different initial conditions. (d) Trajectories starting from 50 different initial conditions for $N = 64$.

N_1). Because the interaction function (Eq. (3)) is an odd function, the phase difference between two clusters is π independent of the population ratio and the stability is given as [10]

- (v) two-cluster state $(N_1, N - N_1)$: $\lambda_1^{(v)} = a - 2b$ (multiplicity 1) with the eigenvector of the inter-cluster mode; $\lambda_2^{(v)} = -2b + (1 - 2N_1/N)a$ (multiplicity $N_1 - 1$) and $\lambda_3^{(v)} = -2b - (1 - 2N_1/N)a$ (multiplicity $N - N_1 - 1$) with the eigenvectors of the intra-cluster modes.

Thus, for the parameter values under consideration, the two-cluster states are saddle solutions. Fig. 9d displays trajectories starting from 50 initial conditions. As seen, the trajectories are similar to those for $N = 4$. The system approaches not only the balanced two-cluster state, namely $(1, 0)$, but also to various two-cluster states. In many cases, R_2 gets large faster than R_1 , implying the formation of nearly balanced two clusters.

4. Concluding remarks

We have studied the effects of pulse stimulations on the dynamics of populations of relaxation oscillators.

Similar to experiments of pulse stimulations on populations of smooth electrochemical oscillators [22], we found the existence of a vulnerable phase in a synchronized population of relaxation oscillators. When pulses are administered at this vulnerable phase, suppression of the collective oscillations as well as formation of (new) clusters can occur in the perturbed populations. In weakly relaxational oscillators, effective desynchronization can be achieved with pulse stimulations by forming transient clusters; repeated application of the pulse can permanently maintain the system in a low-order state. In moderately relaxational oscillators, itinerant clusters are found with pulse stimulations: during the

resynchronization process the system iterates among various cluster states until the globally stable one-cluster state is attained. In populations of globally coupled strongly relaxational oscillators, pulse stimulations at the vulnerable phase did not result in effective desynchronization. Instead, clustering configurations can be induced, which otherwise cannot be obtained easily (e.g., with changes in coupling strength). With repeated pulse administration, a stable two-cluster state that is specific to the pulse administered at the vulnerable phase was attained.

The experimental desynchronization by the formation of clusters with pulse stimuli in relaxational populations is similar to the clustering in desynchronization of N globally coupled logistic maps by decreasing the coupling strength or increasing the nonlinearity parameter of the individual map [30]. In the theoretical studies, it is found that strongly asymmetric two-cluster states are generally first to stabilize when reducing the coupling strength. In our experiments we also found usually a strongly asymmetric clustering state is induced by the first pulse stimulation.

The interaction function of a relaxational oscillator usually contains higher harmonic component [18] which endows the possibility of clustering to the coupled oscillator population [31,10]. We developed a simple phase model that reproduces the occurrence of transient two clusters. The phase model includes first and second harmonics in the interaction function. In the phase model, the transient two-cluster states are saddle states with fast, strongly stable intra-cluster manifold and with slow, weakly unstable inter-cluster manifold. During the motion along the unstable manifold the phase difference among the oscillators is slowly decreasing until the one-cluster state is reached. The transition from a two-cluster saddle state to one-cluster attractor thus

does not necessarily occur through desynchronization. Such transition should be considered for construction of desynchronization methods through coordinated reset of subpopulation [32,33] where it has been generally assumed that the transition from two anti-phase subpopulations to the stable one-cluster state occurs through desynchronization.

For strongly relaxational oscillators, pulse stimulations offer another method to induce clustering states in the system besides global feedback [34–37] and periodic forcing [38,39] that were previously studied. In particular, control of clustering can be achieved with pulse stimulations because the experimental results indicate that a stable specific clustering state can be attained with a specific pulse; this would be useful in relevant fields when the functional role of groups of oscillators that are entrained is addressed, for example, in circadian rhythms [40], biological cell differentiation [41], and multimode laser systems [42].

Acknowledgments

We convey our very best wishes to Stefan Müller on the occasion of his 60th birthday. This work was supported by the National Science Foundation (CBET-0730597).

References

- [1] H. Haken, *Advanced Synergetics*, Springer, Berlin, 1983.
- [2] Y. Kuramoto, *Chemical Oscillations, Waves, and Turbulence*, Springer-Verlag, Berlin, 1984.
- [3] A.T. Winfree, *The Geometry of Biological Time*, Springer-Verlag, New York, 1980.
- [4] A.B. Neiman, D.F. Russell, Synchronization of noise-induced bursts in noncoupled sensory neurons, *Phys. Rev. Lett.* 88 (13) (2002) 138103.
- [5] S. Dano, F. Hynne, S. De Monte, F. d'Ovidio, P.G. Sorensen, H. Westerhoff, Synchronization of glycolytic oscillations in a yeast cell population, *Faraday Discuss.* 120 (2001) 261–276.
- [6] M. Steriade, E.G. Jones, R.R. Llinas, *Thalamic Oscillations and Signaling*, John Wiley & Sons, New York, 1990.
- [7] P.A. Tass, *Phase Resetting in Medicine and Biology. Stochastic Modeling and Data Analysis*, Springer, Berlin, 1999.
- [8] M.G. Rosenblum, A.S. Pikovsky, Controlling synchronization in an ensemble of globally coupled oscillators, *Phys. Rev. Lett.* 92 (11) (2004) 114102.
- [9] M. Rosenblum, A. Pikovsky, Delayed feedback control of collective synchrony: An approach to suppression of pathological brain rhythms, *Phys. Rev. E* 70 (4) (2004) 041904.
- [10] K. Okuda, Variety and generality of clustering in globally coupled oscillators, *Physica D* 63 (3–4) (1993) 424–436.
- [11] D. Golomb, D. Hansel, B. Shraiman, H. Sompolinsky, Clustering in globally coupled phase oscillators, *Phys. Rev. A* 45 (6) (1992) 3516–3530.
- [12] S.C. Manrubia, A.S. Mikhailov, D.H. Zanette, *Emergence of Dynamical Order: Synchronization Phenomena in Complex Systems*, World Scientific, Singapore, 2004.
- [13] M. Banaji, Strongly asymmetric clustering in systems of phase oscillators, *Phys. Rev. E* 71 (2005) 016212.
- [14] V.K. Vanag, L.F. Yang, M. Dolnik, A.M. Zhabotinsky, I.R. Epstein, Oscillatory cluster patterns in a homogeneous chemical system with global feedback, *Nature* 406 (2000) 389–391.
- [15] M. Bertram, C. Beta, M. Pollmann, A.S. Mikhailov, H.H. Rotermund, G. Ertl, Pattern formation on the edge of chaos: Experiments with co-oxidation on a Pt(110) surface under global delayed feedback, *Phys. Rev. E* 67 (3) (2003) 036208.
- [16] A.F. Taylor, P. Kapetanopoulos, B.J. Whitaker, R. Tóth, L. Bull, M.R. Tinsley, Clusters and switchers in globally coupled photochemical oscillators, *Phys. Rev. Lett.* 100 (21) (2008) 214101.
- [17] I.Z. Kiss, W. Wang, J.L. Hudson, Experiments on arrays of globally coupled periodic electrochemical oscillators, *J. Phys. Chem. B* 103 (1999) 11433–11444.
- [18] I.Z. Kiss, Y. Zhai, J.L. Hudson, Predicting mutual entrainment of oscillators with experimental-based phase models, *Phys. Rev. Lett.* 94 (2005) 248301.
- [19] H. Varela, C. Beta, A. Bonnefont, K. Krischer, A hierarchy of global coupling induced cluster patterns during the oscillatory h₂-electrooxidation reaction on a Pt ring-electrode, *Phys. Chem. Chem. Phys.* 7 (2005) 2429–2439.
- [20] P.A. Tass, Effective desynchronization by means of double-pulse phase resetting, *Europhys. Lett.* 53 (1) (2001) 15–21.
- [21] P.A. Tass, Effective desynchronization with bipolar double-pulse stimulation, *Phys. Rev. E* 66 (2002) 036226.
- [22] Y.M. Zhai, I.Z. Kiss, P.A. Tass, J.L. Hudson, Desynchronization of coupled electrochemical oscillators with pulse stimulations, *Phys. Rev. E* 71 (6) (2005) 065202.
- [23] W. Wang, I.Z. Kiss, J.L. Hudson, Experiments on arrays of globally coupled chaotic electrochemical oscillators: Synchronization and clustering, *Chaos* 10 (2000) 248–256.
- [24] A.S. Pikovsky, M.G. Rosenblum, G.V. Osipov, J. Kurths, Phase synchronization of chaotic oscillators by external driving, *Physica D* 104 (1997) 219–238.
- [25] I.Z. Kiss, Y.M. Zhai, J.L. Hudson, Emerging coherence in a population of chemical oscillators, *Science* 296 (2002) 1676–1678.
- [26] Y.M. Zhai, I.Z. Kiss, H. Daido, J.L. Hudson, Extracting order parameters from global measurements with application to coupled electrochemical oscillators, *Physica D* 199 (3–4) (2004) 387–399.
- [27] Y.M. Zhai, I.Z. Kiss, J.L. Hudson, Emerging coherence of oscillating chemical reactions on arrays: Experiments and simulations, *Ind. Eng. Chem. Res.* 43 (2004) 315–326.
- [28] I.Z. Kiss, Y.M. Zhai, J.L. Hudson, Characteristics of cluster formation in a population of globally coupled electrochemical oscillators: An experiment-based phase model approach, *Progr. Theoret. Phys. Suppl.* 161 (2006) 99–106.
- [29] P.A. Tass, Effective desynchronization with a stimulation technique based on soft phase resetting, *Europhys. Lett.* 57 (2002) 164–170.
- [30] O. Popovych, Y. Maistrenko, E. Mosekilde, Role of asymmetric clusters in desynchronization of coherent motion, *Phys. Lett. A* 302 (4) (2002) 171–181.
- [31] H. Daido, Multibranch entrainment and scaling in large populations of coupled oscillators, *Phys. Rev. Lett.* 77 (7) (1996) 1406–1409.
- [32] P.A. Tass, Desynchronization by means of a coordinated reset of neural sub-populations – A novel technique for demand-controlled deep brain stimulation, *Progr. Theoret. Phys. Suppl.* (2003) 281–296.
- [33] P.A. Tass, A model of desynchronizing deep brain stimulation with a demand-controlled coordinated reset of neural subpopulations, *Biol. Cybern.* 89 (2) (2003) 81–88.
- [34] W. Wang, I.Z. Kiss, J.L. Hudson, Synchronization and clustering of arrays of electrochemical oscillators with global feedback, *Ind. Eng. Chem. Res.* 41 (2002) 330–338.
- [35] I.Z. Kiss, C.G. Rusin, H. Kori, J.L. Hudson, Engineering complex dynamical structures: Sequential patterns and desynchronization, *Science* 316 (2007) 1886–1889.
- [36] H. Kori, C.G. Rusin, I.Z. Kiss, J.L. Hudson, Synchronization engineering: Theoretical framework and application to dynamical clustering, *Chaos* 18 (2) (2008) 026111.
- [37] Y. Zhai, I.Z. Kiss, J.L. Hudson, Control of complex dynamics with time-delayed feedback in populations of chemical oscillators: Desynchronization and clustering, *Ind. Eng. Chem. Res.* 47 (10) (2008) 3502–3514.
- [38] W. Wang, I.Z. Kiss, J.L. Hudson, Clustering of arrays of chaotic chemical oscillators by feedback and forcing, *Phys. Rev. Lett.* 86 (2001) 4954–4957.
- [39] I.Z. Kiss, Y. Zhai, J.L. Hudson, Resonance clustering in globally coupled electrochemical oscillators with external forcing, *Phys. Rev. E* 77 (4) (2008) 046204.
- [40] H. Ukai, T.J. Kobayashi, M. Nagano, K.-H. Masumoto, M. Sujino, T. Kondo, K. Yagita, Y. Shigeyoshi, H.R. Ueda, Melanopsin-dependent photo-perturbation reveals desynchronization underlying the singularity of mammalian circadian clocks, *Nature Cell Biol.* 9 (11) (2007) 1327–1334.
- [41] K. Kaneko, Coupled maps with growth and death: An approach to cell differentiation, *Physica D* 103 (1–4) (1997) 505–527.
- [42] K. Wiesenfeld, C. Bracikowski, G. James, R. Roy, Observation of antiphase states in a multimode laser, *Phys. Rev. Lett.* 65 (14) (1990) 1749–1752.